IEEJ Transactions on Industry Applications
Vol.140 No.2 pp.1–8 DOI: 10.1541/ieejias.140.1

Paper

Simple Tuning and Low-Computational-Cost Controller for Enhancing Energy Efficiency of Autonomous-Driving Electric Vehicles

Mitsuhiro Hattori*a) Student Member, Hiroshi Fujimoto*b) Senior Member
Yoichi Hori* Fellow, Yusuke Takeda** Non-member
Koji Sato** Non-member

(Manuscript received xxx,, revised xxx,)

Previous studies have proposed various optimization algorithms, such as dynamic programming (DP) and model predictive control (MPC), to reduce the energy consumption of autonomous-driving vehicles. The difficulties in the industrial applications of these methods are their computational costs and tuning parameters. In this paper, we propose a linear quadratic regulator (LQR), a low-computational-cost algorithm. The proposed controller calculates the input within a sampling period of 10 kHz. By the approximated linear-parameter-varying (LPV) modeling of a vehicle and a motor, we considered the energy loss in the cost function of the LQR. Thus, the proposed method had only one tuning parameter. The effect of changing this parameter, the solver of the LQR for the LPV model, and the influence of the approximation of the models were analyzed. We compared the proposed LQR and DP using computer simulations, a simulation bench, and field experiments. Based on these comparisons, the validity of the proposed method for enhancing the energy efficiency for industrial applications without additional computational hardware was demonstrated.

Keywords: electric vehicle, energy efficiency, autonomous driving, linear quadratic regulator, linear parameter varying system

1. Introduction

1.1 Driver-Assistance System Yearly in road accidents, there are nearly 20–50 million people suffering injuries [1]. Numerous devices, such as disk brakes, seat belts, and airbags, have been developed to provide road safety. In the 1990s, with the advancements in sensors and computers, anti-lock braking systems (ABS) and electronic stabilization programs (ESP) were realized [2]. Using sensors for monitoring the outside of a vehicle, other assistance systems, such as auto-braking and lane departure warning, have also been developed. These systems are called advanced driver-assistance systems (ADAS). In particular, adaptive cruise control (ACC) was developed to maintain a safe, preset distance between cars in a particular lane [3][4]. Because ACC enables a vehicle to operate without the input of the driver, it leads to a highly energy-efficient driving experience [5].

1.2 Energy-Efficient Driving Energy-efficient driving technologies are essential for three reasons: range extension, reducing CO_2 emission, and decreasing the running cost. Range extension is particularly important for electric vehicles, whose cruising distances per supply are relatively shorter than those of gasoline vehicles [6]. From environmental aspects, energy-efficient driving has the potential to significantly reduce CO_2 emissions, which is advantageous because the transportation sector contributes 24% of the global CO_2 emissions from fuel combustion [7]. Furthermore, from an economic perspective, increasing the energy efficiency of a vehicle reduces the running cost, which is gaining increasing dominance in shared economies [8]. Therefore, achieving energy-efficient driving is becoming extremely critical. In this study, energy-efficient driving was achieved by optimal velocity control and reducing the energy loss.

Fig. 1. Picture of FPEV2-Kanon, an experimental vehicle manufactured by our group. In this study, this vehicle was used in the experiments and simulations.

1.3 Previous Research The energy loss of electric vehicles consists of electrical loss and dynamical loss. The copper loss and iron loss of a motor contribute to the electrical loss, and dragging forces, such as air resistance, viscous resistance, and rolling friction, cause the dynamical loss. In this study, we reduce all the losses together by achieving optimal acceleration and deceleration. Our research group has previously published a paper on reducing energy consumption with consideration of the ride comfort [9]; however, we

a) Correspondence to: hattori.mitsuhiro18@ae.k.u-tokyo.ac.jp
b) Correspondence to: fujimoto@k.u-tokyo.ac.jp
* The University of Tokyo
5–1–5, Kashiwanoha, Kashiwa, Chiba, 227–8561 Japan
** ONO SOKKI CO., LTD.
3–9–3, Shin-Yokohama, Kohoku-ku, Yokohama, Kanagawa, 222–8507 Japan

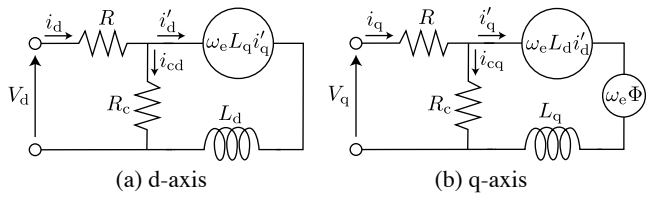

(a) d-axis (b) q-axis

Fig. 2. Equivalent circuit of a permanent magnet synchronous motor (PMSM).

did not consider this in the present study, and mainly focused on simple tuning and the computational cost.

Previous studies have proposed various optimal control techniques to reduce the energy consumption of a vehicle by achieving autonomous driving. The gradient method is an optimization method with precomputation. It calculates the optimal input before driving and applies a feedforward control [10]. This method needs consideration of the vehicle control, which is significantly affected by the disturbance.

Dynamic programming (DP) is a feedback control with a calculated table of inputs. Autonomous-driving trains widely use this method for reducing the energy consumption [11][12]. For electric vehicles, DP is also employed to calculate the optimal velocity trajectory [13][14]. DP is a global optimization algorithm and can easily deal with constraints. DP typically yields the best results among the various methods; however, the size of the calculated table is extremely large to support the various scenarios of a vehicle.

Model predictive control (MPC) is an online optimization control that predicts a future state. MPC is widely used to reduce the energy consumption of vehicles [15][16]. In MPC, it is challenging to complete the computations in the step period because of the complexity of the optimization. To solve this problem, methods such as considering the constraints with a reference governor [17], and combining with the precomputation of DP [18] have been proposed. However, it is still challenging to tune the parameters of the cost function for MPC.

These methods are not typically chosen because of the limitation of the production costs. Our experimental vehicle has sufficient memory and computing power, which typical production cars do not possess. For these cars, this low-computational-cost controller would be a good option, and therefore, this research is important. In this paper, we proposed a low-computational-cost algorithm for applying to real vehicle control.

1.4 Contribution In this study, we used a linear quadratic regulator (LQR) as an optimization algorithm having a low computational cost. The proposed controller operates without expensive memory or computer requirements and calculates the input in a sampling period of 10 kHz. Previous studies with LQRs considered the weight of the cost function and its value in the control system as the tuning parameters. Thus, an LQR is currently challenging to design [19][20]. To solve this problem, we designed an LQR controller with only one tuning parameter. With appropriate approximations, we considered the energy loss of an electric vehicle as the cost function of the LQR. Furthermore, we analyzed the parameter both quantitatively and qualitatively.

In this study, we compared the proposed method with DP, which is a global optimization algorithm. We evaluated the methods by not only computer simulations but also by experiments on a test bench and in a test field with our vehicle, FPEV2-Kanon, which is shown in Fig. 1. By linear-parameter-varying (LPV) modeling of the vehicle and the motor, the energy consumption was improved.

Table 1. Parameters of the motors. The parameters are different for the front wheel and the rear wheel.

Parameter	Description	Front	Rear
J_ω	Wheel inertia	1.24 kgm^2	1.26 kgm^2
L_q	q-axis inductance	0.69 mH	2.34 mH
Φ	Leakage flux	0.18 Wb	0.249 Wb
R	Copper resistance	0.0602 Ω	0.1036 Ω
R_{c0}	Equivalent iron loss resistance	55 Ω	454.23 Ω
R_{c1}	Equivalent iron loss resistance	0.14 Ω	0.1516 Ω
K_t	Motor constant	2.7 Nm/A	1.245 Nm/A
P_n	Number of pole pairs	20/2	20/2

The remainder of this paper is as follows. Section 2 describes the experimental vehicle and its model, and Section 3 presents the details of the proposed LQR controller design and comparison with the DP controller. Section 4 discusses the results of the simulations and experiments and analyzes the parameter, solver, and approximation. Finally, Section 5 concludes this paper.

2. Modeling

2.1 Experimental Vehicle FPEV-2 Kanon, as displaced in Fig. 1, is an experimental vehicle manufactured by our research group. This vehicle has four independently driven in-wheel motors, and the motor is an outer-rotor permanent magnet synchronous motor (PMSM). Because all the in-wheel motors are direct-drive, the reaction force transfers to the road without the effect of the gear backlash or shaft torsion. Therefore, we only considered the loss of the motor and the driving resistance as the energy loss components.

2.2 Power Model of Motor The equivalent circuit of the motor is displayed in Fig. 2. The input power of the motor, P_{in}, is defined as the sum of the output power, P_{out}, copper loss, P_c, and iron loss, P_i. They are

$$P_{out} = \sum_{all} \omega T, \quad P_c = \sum_{all} R\left(\frac{T}{K_t}\right)^2, \quad \cdots\cdots(1)$$

$$P_i = \sum_{all} \frac{\omega P_n}{R_c}\left\{\left(L_q \frac{T}{K_t}\right)^2 + \Phi^2\right\}, \cdots\cdots(2)$$

where T and ω are the torque and rotational speed, respectively, and the equivalent iron loss resistance, R_c is

$$\frac{1}{R_c} = \frac{1}{R_{c0}} + \frac{1}{R_{c1}|\omega P_n|}. \cdots\cdots(3)$$

The parameters of the motor are listed in Table 1.

2.3 Vehicle Dynamics Model The dragging force of the vehicle is described as

$$F_{DR} = \mu_r M g + b|v| + F_a v^2, \cdots\cdots(4)$$

where each term refers to the rolling resistance, viscous resistance, and air resistance. All the parameters are listed in Table 2. The load forces of the front and rear wheels are expressed as follows:

Table 2. Parameters of the vehicle.

Parameter	Description	Value
M	Vehicle mass	880 kg
g	Gravity acceleration	9.8 m/s^2
b	Viscous resistance coefficient	10.7 kg/s
r	Wheel radius	0.302 m
F_a	Air resistance coefficient	0.552 Ns^2/m^2
μ_r	Rolling resistance coefficient	0.0126
h_g	Height of center of gravity (CG)	0.51 m
l_f	Distance between CG & front wheel	1.013 m
l_r	Distance between CG & rear wheel	0.702 m

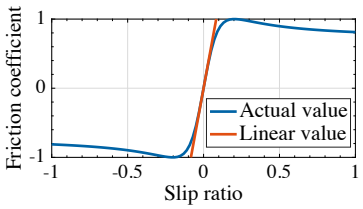

Fig. 3. The relation between the slip ratio and the friction coefficient. The magic formula [21] calculates the actual value. The linear value is calculated with D_s.

$$N_f = \frac{1}{2}\left(\frac{l_r}{l}Mg - \frac{h_g}{l}M\dot{v}\right),\ N_r = \frac{1}{2}\left(\frac{l_f}{l}Mg + \frac{h_g}{l}M\dot{v}\right)\cdots (5)$$

To calculate driving force, slip ratio λ is defined as

$$\lambda = \frac{r\omega - v}{\max(v, r\omega)}, \cdots (6)$$

where ω is the wheel angular velocity. The relation between the road friction coefficient, μ, and the slip ratio, λ, is presented in Fig. 3. With this relation, we can calculate the driving force of each wheel as $F = \mu N$. The equations of the wheel rotation and the vehicle motion are

$$J_\omega \dot{\omega} = T - rF, \quad M\dot{v} = \sum F - F_{DR}, \cdots (7)$$

where T is the torque and F is the driving force of each wheel.

3. Controller

3.1 Previous Approach for Comparison We compare DP with the proposed method because the results with DP are typically the best among those of other methods. DP is a commonly used offline optimization algorithm for trains [12]. DP divides the problem into multiple subproblems, and the optimization is solved efficiently with the results of the subproblems. The problem is discretized by the velocity and the position to apply DP. We approximated the power model of the motor as follows:

$$P_{out} = \frac{1}{2}vF_{all}\sum\left(1 + \frac{F_{all}}{4D_sN}\right), \cdots (8)$$

$$P_c = \frac{r^2}{8}F_{all}^2\sum\frac{R}{K_t^2}, \cdots (9)$$

$$P_i = 2\frac{v^2}{r^2}\sum\frac{P_n^2}{R_c}\left\{\left(\frac{rL_qF_{all}}{4K_t}\right)^2 + \Phi^2\right\}, \cdots (10)$$

to calculate the power from the discretized velocity. F_{all} is the sum of the driving forces, and D_s(= 12) is the driving stiffness, which is visualized in Fig. 3.

In this approach, the velocity of the vehicle is optimized.

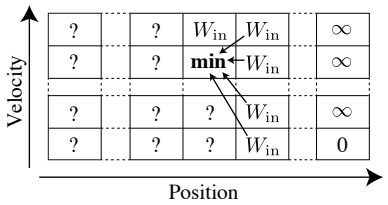

Fig. 4. The algorithm of DP. From the final position and velocity, the optimal velocity is calculated backward.

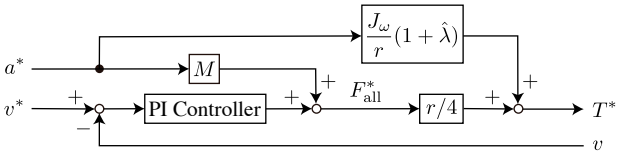

Fig. 5. Block diagram of the velocity controller. This controller was used in a previous approach of DP.

The optimization algorithm is presented in Fig. 4. The evaluation function is the energy consumption, W_{in}, which is the time integration of P_{in}(= P_{out} + P_c + P_i). DP calculates the optimal velocity for each position by setting the value of the goal to 0 if the velocity is 0 m/s and to ∞ if it is not. Using the result of the next step, DP determines the minimum value of the evaluation function in each step and calculates the optimal velocity of each position in the table.

Using the calculated velocity trajectory, the vehicle is controlled to follow the velocity, v^*, and its acceleration, a^*. The velocity controller is shown in Fig. 5. In this case, $\lambda^* = 0.05$ and the gains of the PI controller are set as $K_p = 10M$ and $K_i = 25M$. Specifically, the pole is set as -5 rad/s for the plant $sMv = F$. Using the controller, the inverter torque input, T^*, is calculated. The details of this approach are presented in a previously published article of our group [22]. Because creating a table in DP under numerous conditions is impractical, the table in this study is limited to the problem establishment used in this paper. Nevertheless, the computational time to form the table is more than a few minutes.

3.2 Linear-Parameter-Varying Model In this study, the LQR was used to optimize the energy consumption. To apply the LQR, we approximated the driving resistance as a first-order equation,

$$F_{DR} = \mu_r Mg + b|v| + F_a v^2 \approx A + Bv, \cdots (11)$$

where A and B are the driving resistance coefficients. In this study, the proposed method approximated the driving resistance every step as a linearization around the state at the step. The linearization is displayed in Fig. 6. The coefficient B is

$$B(v') = b + 2F_a v', \cdots (12)$$

where v' is the velocity at the step. Thus, the model is described as an LPV model of the vehicle velocity, v.

3.3 Controller Design The linearized driving resistance coefficient, B, simplifies the vehicle model as

$$M\frac{dv}{dt} = F_{all} - B(v)v, \cdots (13)$$

where F_{all} is the sum of the driving forces of the four wheels. Because the energy loss from the wheel slip is negligible, the

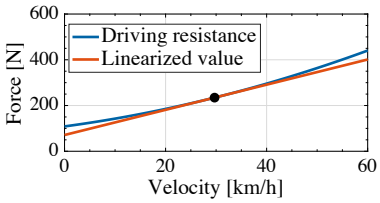

Fig. 6. The linearization of the driving resistance. In this figure, the velocity at the step of the linearization is 30 km/h.

wheel slip is ignored, and

$$rF_{\text{all}} = \sum_{\text{all}} T = \sum_{\text{all}} K_{\text{t}} i = 4K_{\text{t}} i \cdots\cdots\cdots\cdots\cdots\cdots (14)$$

is formulated. T and i are the torque and current of the motor, respectively, and K_{t} is the motor coefficient. Using this equation, equation (13) becomes

$$M\frac{dv}{dt} = \frac{4K_{\text{t}} i}{r} - B(v)v \cdots\cdots\cdots\cdots\cdots\cdots\cdots\cdots (15)$$

and is described with the input current, i, of the motor and velocity, v, of the vehicle.

To apply the LQR, the circuit equation of the motor is approximated as

$$L\frac{di}{dt} = V - Ri - K_{\text{e}}\omega, \cdots\cdots\cdots\cdots\cdots\cdots\cdots\cdots (16)$$

which ignores the iron loss and only considers the copper loss. In this equation, V is the voltage, K_{e} is back electromotive force constant, and R is the copper loss resistance. Ignoring the wheel slip and assuming $v = r\omega$, equation (16) is rewritten as

$$L\frac{di}{dt} = V - Ri - \frac{K_{\text{e}} v}{r}, \cdots\cdots\cdots\cdots\cdots\cdots\cdots\cdots (17)$$

and also described with i and v. The velocity and position errors caused by ignoring the wheel slip are less than 1 %, which value is acceptable for daily driving.

Using these formulations, calculating (15) $\times\, v$ + (17) $\times\, 4i$ and assuming $K_{\text{t}} = K_{\text{e}}$ lead to

$$\frac{d}{dt}\left(\frac{1}{2}Mv^2 + 4\frac{1}{2}Li^2\right) = 4Vi - (4Ri^2 + Bv^2). \cdots\cdots (18)$$

The right side of equation (18) consists of the output power, Vi, copper loss, Ri^2, and driving resistance, Bv^2. Thus, the objective should be minimizing the loss term, $4Ri^2 + Bv^2$.

In the LQR, the state space system is

$$\frac{d\boldsymbol{x}}{dt} = \begin{pmatrix} 0 & 1 \\ 0 & -\frac{B}{M} \end{pmatrix}\boldsymbol{x} + \begin{pmatrix} 0 \\ \frac{4K_{\text{t}}}{rM} \end{pmatrix}\boldsymbol{u}, \cdots\cdots\cdots\cdots\cdots\cdots (19)$$

where the state, $\boldsymbol{x} = (p \;\; v)^T$, consists of the position, p, and velocity, v, and the input $\boldsymbol{u} = i^*$ is the current reference. Here, the current control of the inverter is assumed as ideal.

The evaluation function of the LQR is

$$J(\boldsymbol{u}) = \int_0^\infty (\boldsymbol{x}^T\boldsymbol{Q}\boldsymbol{x} + \boldsymbol{u}^T\boldsymbol{R}\boldsymbol{u})dt, \cdots\cdots\cdots\cdots\cdots\cdots (20)$$

and by setting the weights, $\boldsymbol{Q}$ and $\boldsymbol{R}$, as

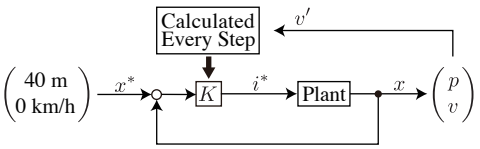

Fig. 7. Block diagram of the controller. In this case, the vehicle stops at 40 m.

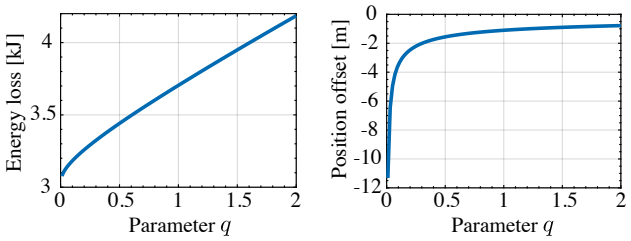

(a) Energy loss. (b) Position offset.

Fig. 8. The effect of changing the parameter, q. Parameter q to (a) the energy loss and (b) the position offset.

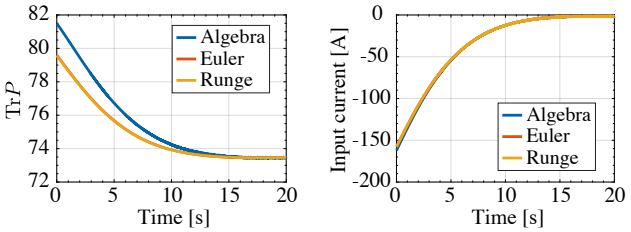

(a) Trace of P. (b) Calculated input.

Fig. 9. Simulation results with different solvers. Algebra is the result of the proposed method, and Euler and Runge are the results of the differential equation. (a) Trace of calculated P is different in the proposed method. (b) Calculated inputs are close to each other.

$$\boldsymbol{Q} = \begin{pmatrix} q & 0 \\ 0 & B \end{pmatrix}, \quad \boldsymbol{R} = 4R, \cdots\cdots\cdots\cdots\cdots\cdots (21)$$

the function to be integrated in equation (20) is converted to

$$\boldsymbol{x}^T\boldsymbol{Q}\boldsymbol{x} + \boldsymbol{u}^T\boldsymbol{R}\boldsymbol{u} = qp^2 + Bv^2 + 4Ri^2, \cdots\cdots\cdots\cdots (22)$$

where q is the only parameter to be tuned. Thus, the minimization of the evaluation function is equivalent to the minimization of the energy loss, $Bv^2 + 4Ri^2$, and position error, qp^2. With this formulation of the LQR, the controller calculates the optimal feedback gain, K, every step. Fig. 7 presents the block diagram of this controller.

3.4 Parameter Tuning Method In the proposed controller, the only parameter to be tuned is q. This parameter is required to reduce the offset of the position. Considering the friction of a road, we simulated the offset with different q, and determined the relations between the values of the energy loss, $Bv^2 + 4Ri^2$, and q. The relations are shown in Fig. 8. A larger q results in a smaller offset but leads to more energy consumption. With these relations, a designer can determine the parameter, q. For example, if a designer allows a position offset of 1 m, then the parameter is tuned as $q = 1.0$. This value is used in the simulations and experiments.

3.5 Low-Computational-Cost Solver For a time-variant system and the cost function,

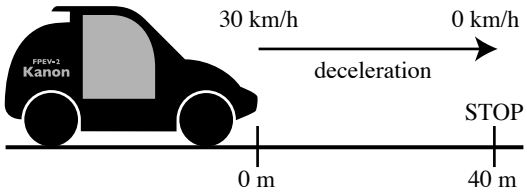

Fig. 10. Illustration of the problem establishment. The vehicle decelerates from 30 km/h and stops at 40 m.

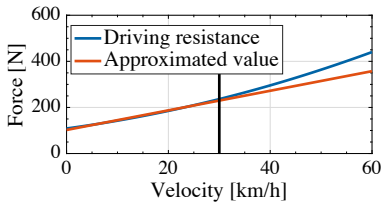

Fig. 11. First-order approximation of the driving resistance used in the LTI model. In this figure, the velocity range is from 0 km/h to 30 km/h.

$$\dot{\boldsymbol{x}} = \boldsymbol{A}(t)\boldsymbol{x} + \boldsymbol{B}(t)\boldsymbol{u}, \quad \boldsymbol{x}(0) = x_0, \cdots\cdots\cdots\cdots (23)$$

$$J(\boldsymbol{u}) = \int_0^\infty (\boldsymbol{x}^T\boldsymbol{Q}(t)\boldsymbol{x} + \boldsymbol{u}^T\boldsymbol{R}(t)\boldsymbol{u})dt, \cdots\cdots\cdots\cdots (24)$$

it is generally required to solve Riccati differential equation

$$\boldsymbol{A}^{\mathrm{T}}\boldsymbol{P} + \boldsymbol{P}\boldsymbol{A} - \boldsymbol{P}\boldsymbol{B}\boldsymbol{R}^{-1}\boldsymbol{B}^{\mathrm{T}}\boldsymbol{P} + \boldsymbol{Q} = -\dot{\boldsymbol{P}}. \cdots\cdots\cdots\cdots (25)$$

To solve the above numerically, the Euler method and the Runge–Kutta method are widely used. However, solving with these methods requires a high computational cost. In this study, we assumed $\dot{\boldsymbol{P}} = 0$ for every step and solved the algebraic Riccati equation,

$$\boldsymbol{A}^{\mathrm{T}}\boldsymbol{P} + \boldsymbol{P}\boldsymbol{A} - \boldsymbol{P}\boldsymbol{B}\boldsymbol{R}^{-1}\boldsymbol{B}^{\mathrm{T}}\boldsymbol{P} + \boldsymbol{Q} = 0. \cdots\cdots\cdots\cdots (26)$$

The effect of assuming $\dot{\boldsymbol{P}} = 0$ was estimated and displayed in Fig. 9. Algebra is the result of solving the algebraic Riccati equation, and Euler and Runge are the results of solving the Riccati differential equation with the Euler method and the Runge–Kutta method, respectively. With these methods, P is computed backward from the final state. This simulation uses the actual simulation result of the vehicle for the values of the position and velocity for each step.

Fig. 9 (a) shows the trace of P. P is almost the same with the Euler method and the Runge–Kutta method, but is different with the algebraic Riccati equation. In Fig. 9 (b), however, the calculated current inputs of the controller by all the solvers are sufficiently close. The input is almost the same with the algebraic Riccati equation because the inputs from the position error and velocity error canceled each other.

Because the system is second order, the positive definite solution, P, of equation (26) can be solved analytically. Using P, the feedback gain of the controller is calculated as $\boldsymbol{K} = -\boldsymbol{R}^{-1}\boldsymbol{B}^{\mathrm{T}}\boldsymbol{P}$, and the controller input is $\boldsymbol{u} = \boldsymbol{K}\boldsymbol{x}$. Because the calculation only involves some multiplication and solving a quadratic equation, the proposed controller completes the computation within a sampling period of 10 kHz.

4. Evaluation

4.1 Problem Establishment For evaluation, we cannot use a driving pattern such as the JC08 mode because these methods change the velocity trajectory. Thus, the problem establishment for evaluating the proposed method is a simple decelerating case, as shown in Fig. 10. The reason to use this is that the share of reducing the energy consumption here is relatively large. In this deceleration, the objectives are to maximize the regenerative energy and minimize the energy consumption. To evaluate the proposed method of the LPV model, we compared DP, as introduced in 3.1, and a linear-time-invariant (LTI) model of the proposed method. The regenerative energy of the DP is the best theoretically.

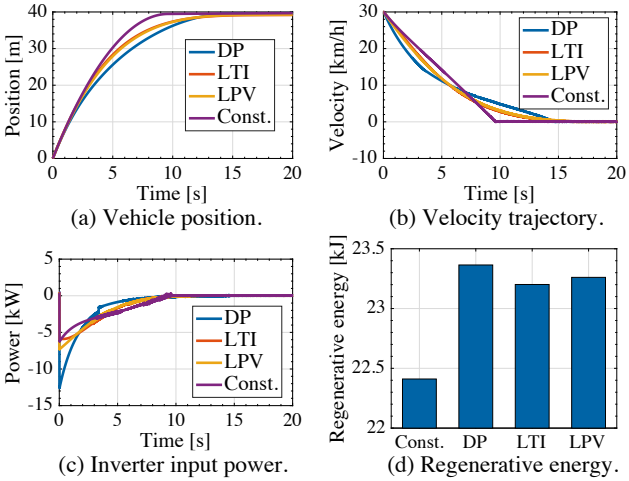

Fig. 12. Simulation results (parameter $q = 1.0$). The vehicle decelerates from 30 km/h and stops at 40 m.

The regenerative energies of other methods, such as MPC, are between those of the DP and our proposed method. In the proposed method of LPV, we linearized the driving resistance every step around the state at the step, and in the LTI model, the driving resistance was approximated as a first-order approximation with the least square method. The approximation for the LTI model is displayed in Fig. 11.

4.2 Computer Simulations For the computer simulations, we used a full vehicle model of the experimental vehicle. This model had a tire model with the slip ratio and characteristic of the motor and a vehicle model with the load distribution of the four wheels. Vehicle control of each optimization algorithm is simulated with this model and compared in terms of the energy consumption. For only the simulation, we also compared constant-acceleration control.

The comparison of the methods is presented in Fig. 12. Using the method described in 3.4, parameter q was tuned to 1.0. In Fig. 12, Const. refers to the constant-acceleration control. Compared to the constant-acceleration control, DP, LTI, and LPV are more than 3% better in terms of the regenerative energy. The proposed LPV controller regenerates more energy than constant-parameter LTI.

4.3 Energy Loss Separation The energy loss from the simulation is separated to analyze the energy consumption of each method. The energy loss is divided into air resistance W_{a}, viscous resistance W_{v}, rolling friction W_{r}, copper loss W_{c}, and iron loss W_{i}, which are calculated as

$$W_{\mathrm{a}} = \int F_{\mathrm{a}} v^3 dt, \quad W_{\mathrm{v}} = \int b v^2 dt, \quad W_{\mathrm{r}} = \int \mu_{\mathrm{r}} M g v dt,$$

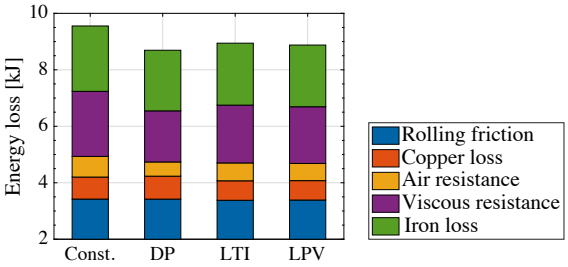

Fig. 13. Simulation result of the loss separation. Compared to DP, the proposed method reduces the copper loss more, whereas it increases the driving resistance.

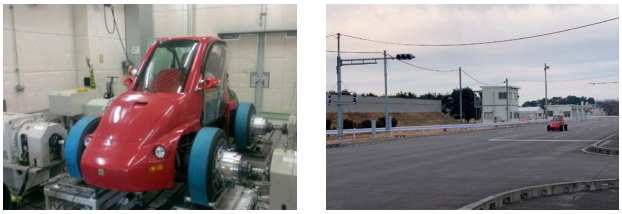

(a) Simulation bench. (b) Experimental field.

Fig. 14. Pictures of the evaluation using the experimental vehicle. (a) Simulation bench of ONO SOKKI CO., LTD. (b) Experimental field of the Japan Automobile Research Institute (JARI).

$$W_c = \int P_c dt, \quad W_i = \int P_i dt. \quad \cdots\cdots\cdots\cdots\cdots\cdots \quad (27)$$

The result of the loss separation is presented in Fig. 13. This uses the simulation result in Fig. 12. Because the rolling friction is precisely the same for all the methods, the figure omits the range of 0 kJ–2 kJ. Compared to DP, the proposed method reduces the copper loss more, whereas it increases the energy loss from the driving resistance.

4.4 Bench Test The real car simulation bench (RC-S) shown in Fig. 14 (a) is an instrument of ONO SOKKI CO., LTD. for bench tests using an actual vehicle. Because the RC-S absorbs the driving force by directly connecting the driving wheels to a dynamometer, it can test electric vehicles with a rapid reaction [23]. For the experiment on the bench test, we employed the experimental vehicle, FPEV-2 Kanon. The RC-S calculates the velocity of the vehicle, and the position is calculated as the time integration of the velocity. Under each condition, we conducted five experiments and then calculated the mean and the standard error of the energy consumption.

In this bench test, the rolling friction is set higher than the regular asphalt of the experimental field. The results are shown in Fig. 15. Using the method discussed in 3.4, parameter q was tuned to 1.0. With the proposed LPV control, the vehicle regenerates more energy than DP in this bench test. However, the vehicle with the proposed method did not reach 40 m in this bench test, because of the high rolling friction of the road.

4.5 Field Experiment We used the city course of the Japan Automobile Research Institute (JARI) and our experimental vehicle FPEV2-Kanon, in the field experiment. Under each condition, we conducted five experiments and calculated the standard error of the energy consumption. Ignoring the wheel slip, we used a wheel resolver to measure the velocity of the vehicle and calculated the position as the time integration of the velocity. This is acceptable because the difference between the true position and the calculated position in the bench test was less than 1 %. Thus, the only sensor used to control was the wheel resolver. We calculated the energy consumption as the product of the DC values of the current probe and voltage probe connected to the output of the boost converter.

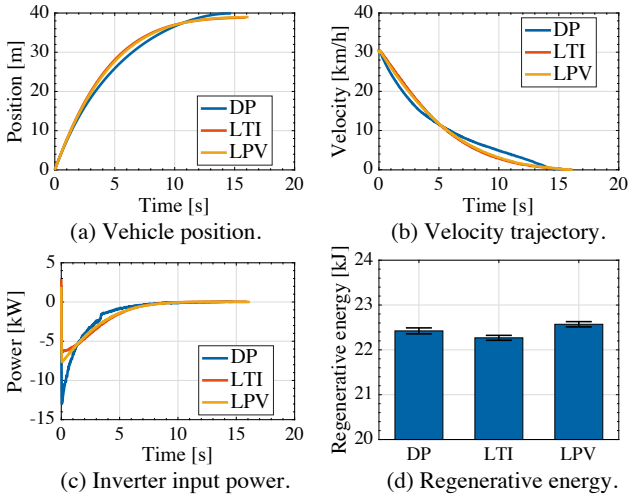

(a) Vehicle position. (b) Velocity trajectory.
(c) Inverter input power. (d) Regenerative energy.

Fig. 15. Results of the bench test (q = 1.0). The vehicle decelerates from 30 km/h and stops at 40 m. DP: 22.42 ± 0.06, LTI: 22.26 ± 0.05, LTI: 22.57 ± 0.05)

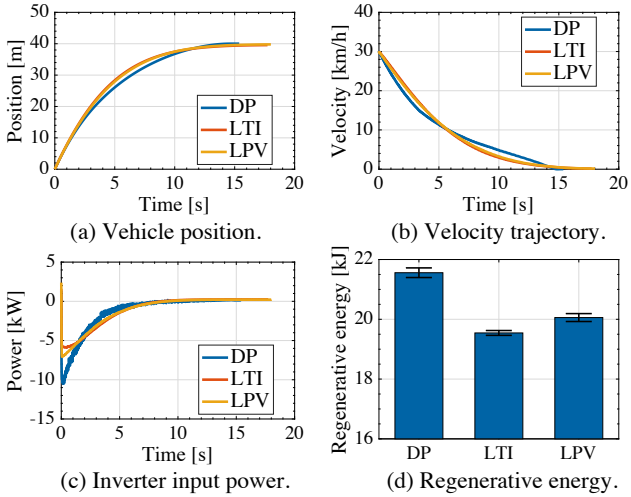

(a) Vehicle position. (b) Velocity trajectory.
(c) Inverter input power. (d) Regenerative energy.

Fig. 16. Results of the field test (q = 1.0). The vehicle decelerates from 30 km/h and stops at 40 m. (DP: 21.55 ± 0.16, LTI: 19.54 ± 0.08, LTI: 20.05 ± 0.13)

Parameter q was tuned with the method presented in 3.4. The experimental results of the field experiment are shown in Figs. 16–18. Figs. 16 and 17 are the results of the deceleration from 30 km/h with different parameters q. Fig. 18 is the result of the deceleration from 45 km/h with a distance of 60 m. Same as in the simulation and bench test results, the proposed LPV regenerates more energy than the constant-parameter LTI.

4.6 Discussion In the proposed LQR, we ignored the wheel slip and iron loss and approximated the driving resistance. The effect of the wheel slip on the energy loss is al-

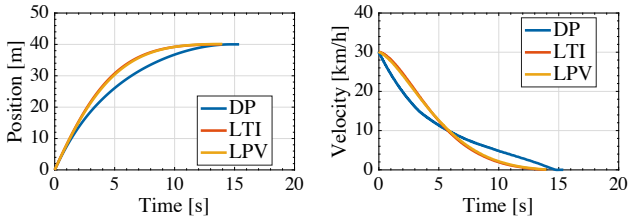

(a) Vehicle position.

(b) Velocity trajectory.

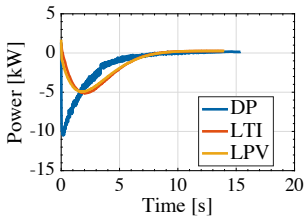

(c) Inverter input power.

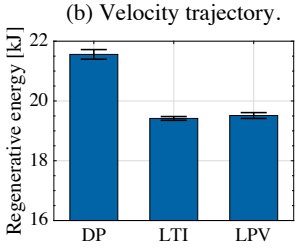

(d) Regenerative energy.

Fig. 17. Results of the field test (q = 2.0). The vehicle decelerates from 30 km/h and stops at 40 m. (DP: 21.55 ± 0.16, LTI: 19.41 ± 0.06, LTI: 19.51 ± 0.09)

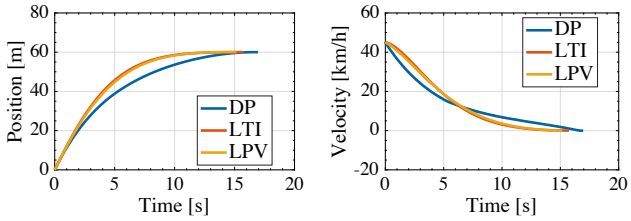

(a) Vehicle position.

(b) Velocity trajectory.

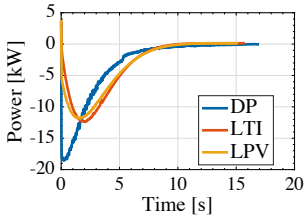

(c) Inverter input power.

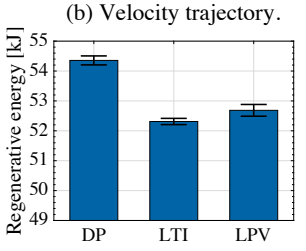

(d) Regenerative energy.

Fig. 18. Results of the field test (q = 2.0). The vehicle decelerates from 45 km/h and stops at 60 m. (DP: 54.35 ± 0.15, LTI: 52.31 ± 0.10, LTI: 52.68 ± 0.19)

ready known to be negligible [10], whereas the iron loss and driving resistance contribute significantly to the energy loss. As shown in Fig. 13, the iron loss does not change much for the different controllers. Thus, ignoring the iron loss in the cost function is acceptable. In the proposed LQR, we considered the copper loss but approximated the driving resistance. The proportion of the copper loss in the cost function is relatively large, and the LQR reduces the current, i of the motor more than DP. This reduces the deceleration and increases the velocity, v. Thus, the loss from the driving resistance increases for the proposed method.

In the proposed method with the LPV model, the approximation of the driving resistance is better than with the LTI model. Therefore, the energy loss in LPV is less than in LTI. Because it is impossible to surpass the result of global optimization DP, the proposed method is valid for reducing the energy consumption of electric vehicles. Regenerative energy of other methods, such as MPC, is in between that of DP and our proposed method. The precalculation of DP requires more than a few minutes for this limited problem establishment but needs a large memory size. The comparison of the computational cost is summarized in Table 3. The proposed method is sufficiently fast to complete the computation without additional computational hardware.

Table 3. Comparison of the computational costs of all the methods. Because the computational cost differs for each environment, only the decades are shown.

Method	Computational Time [μs]	Memory Space [KB]
LQR (Proposed)	10^1	10^0
DP (Compared)	10^2	10^3
MPC (Example)	10^5	10^2

5. Conclusion

Previous studies have proposed various optimization algorithms with different computational costs for the optimization of the energy consumption of vehicles. High computational costs and complex parameter tuning are challenging for industry applications. In this paper, we proposed an LQR as a simple tuning and low-computational-cost controller and compared it with the global optimization algorithm, DP, in terms of energy consumption. With approximations of some conditions, we considered the energy loss of an electric vehicle in the cost function of the LQR, and the LQR was successfully applied to the optimization of the energy consumption of an electric vehicle. The LPV model improved the approximation of the driving force and reduced the energy consumption. The strength of the proposed method is simple tuning and low computational cost, and its regenerative energy is not better than other methods. However, the proposed method is a valid option for industrial applications, because the difficulty of the parameter tuning and hardware cost for the computations are reduced for implementation. Possible future work includes comparison with more optimal control algorithms and consideration of the ride comfort.

Acknowledgment

Industrial Technology Research Grant Program partly supported this research by the New Energy and Industrial Technology Development Organization (NEDO) of Japan (number 05A48701d), the Ministry of Education, Culture, Sports, Science, and Technology grant (number 18H03768 and 26249061), and JST CREST Grant Number JPMJCR15K3, Japan. We would like to thank Editage (www.editage.com) for English language editing.

References

(1) World Health Organization: “Global status report on road safety”, Technical report (2018).
(2) G. Leen and D. Heffernan: “Expanding Automotive Electronic Systems”, Computer, **35**, 1, pp. 88–93 (2002).
(3) W. D. Jones: “Building safer cars”, IEEE Spectrum, **39**, 1, pp. 82–85 (2002).
(4) B. Rouzier, M. Hazaz, T. Murakami and W. Xu: “Application of Active Driving Assist to Remotely Controlled Car in Collision Avoidance”, IEEJ Journal of Industry Applications, **7**, 4, pp. 289–297 (2018).
(5) K. J. Malakorn and B. Park: “Assessment of Mobility, Energy, and Environment Impacts of IntelliDrive-based Cooperative Adaptive Cruise Control and Intelligent Traffic Signal Control”, IEEE International Symposium on Sustainable Systems and Technology, pp. 1–6 (2010).
(6) C. C. Chan: “The State of the Art of Electric, Hybrid, and Fuel Cell Vehi-

cles", Proceedings of the IEEE, **95**, 4, pp. 704–718 (2007).
(7) International Energy Agency: "CO2 Emissions from Fuel Combustion Highlights", Technical report (2017).
(8) F. Bardhi and G. M. Eckhardt: "Access-Based Consumption: The Case of Car Sharing", Journal of Consumer Research, **39**, 4, pp. 881–898 (2012).
(9) T. Fukuda, H. Fujimoto, Y. Hori, D. Kawano, Y. Goto, Y. Takeda and K. Sato: "Range extension autonomous driving of electric vehicle considering maximum jerk constraint", EVS 2017 - 30th International Electric Vehicle Symposium and Exhibition, pp. 1–11 (2017).
(10) Y. Ikezawa, H. Fujimoto, Y. Hori, D. Kawano, Y. Goto, M. Tsuchimoto and K. Sato: "Range Extension Autonomous Driving for Electric Vehicles Based on Optimal Velocity Trajectory Generation and Front-Rear Driving-Braking Force Distribution", IEEJ Journal of Industry Applications, **5**, 3, pp. 228–235 (2016).
(11) H. Ko, T. Koseki and M. Miyatake: "Numerical Study on Dynamic Programming Applied to Optimization of Running Profile of a Train", IEEJ Transactions on Industry Applications, **125**, 12, pp. 1084–1092 (2005).
(12) N. Ghaviha, M. Bohlin, F. Wallin and E. Dahlquist: "Optimal Control of an EMU Using Dynamic Programming", Energy Procedia, Vol. 75, Elsevier B.V., pp. 1913–1919 (2015).
(13) V.-D. Doan, H. Fujimoto, T. Koseki, T. Yasuda, H. Kishi and T. Fujita: "Iterative Dynamic Programming for Optimal Control Problem with Isoperimetric Constraint and Its Application to Optimal Eco-driving Control of Electric Vehicle", IEEJ Journal of Industry Applications, **7**, 1, pp. 80–92 (2018).
(14) Y. Chen, X. Li, C. Wiet and J. Wang: "Energy Management and Driving Strategy for In-Wheel Motor Electric Ground Vehicles With Terrain Profile Preview", IEEE Transactions on Industrial Informatics, **10**, 3, pp. 1938–1947 (2014).
(15) M. Vajedi and N. L. Azad: "Ecological Adaptive Cruise Controller for Plug-In Hybrid Electric Vehicles Using Nonlinear Model Predictive Control", IEEE Transactions on Intelligent Transportation Systems, **17**, 1, pp. 113–122 (2016).
(16) S. Xu and H. Peng: "Design and Comparison of Fuel-Saving Speed Planning Algorithms for Automated Vehicles", IEEE Access, **6**, pp. 9070–9080 (2018).
(17) B. Sakhdari and N. L. Azad: "A Distributed Reference Governor Approach to Ecological Cooperative Adaptive Cruise Control", IEEE Transactions on Intelligent Transportation Systems, **19**, 5, pp. 1496–1507 (2018).
(18) A. Weißmann, D. Görges and X. Lin: "Energy-optimal adaptive cruise control combining model predictive control and dynamic programming", Control Engineering Practice, **72**, pp. 125–137 (2018).
(19) C. Park and H. Lee: "A Study of Adaptive Cruise Control System to Improve Fuel Efficiency", International Journal of Environmental Pollution and Remediation, **5**, pp. 15–19 (2017).
(20) Z. Han, N. Xu, H. Chen, Y. Huang and B. Zhao: "Energy-efficient control of electric vehicles based on linear quadratic regulator and phase plane analysis", Applied Energy, **213**, pp. 639–657 (2018).
(21) H. B. Pacejka and E. Bakker: "Tire and Vehicle Dynamics", Elsevier (2012).
(22) T. Fukuda, H. Fujimoto, Y. Hori, D. Kawano, Y. Goto, Y. Takeda and K. Sato: "Basic Study on Range Extension Autonomous Driving of Electric Vehicle Considering Velocity Constraint for Real-Time Implementation", IEEJ International Workshop on Sensing, Actuation, Motion Control, and Optimization, pp. 1–6 (2017).
(23) Y. Goto, D. Kawano, K. Sato and K. Echigo: "Analysis of Behavior of Fuel Consumption and Exhaust Emissions under On- road Driving Conditions Using Real Car Simulation Bench (RC-S)", SAE International Journal of Engines, **2**, 2, pp. 611–616 (2009).

Mitsuhiro Hattori (Student Member) received his B.E. degree from the Department of Electrical and Electronic Engineering, the University of Tokyo, Japan in 2018. He is currently working toward an M.S. degree at the Department of Advanced Energy, Graduate School of Frontier Sciences, The University of Tokyo. His interests are in control engineering and electric vehicle control. He is a student member of the Institute of Electrical and Electronics Engineers and the Society of Automotive Engineers of Japan.

Hiroshi Fujimoto (Senior Member) received his Ph.D. degree from the Department of Electrical Engineering, the University of Tokyo in 2001. In 2001, he joined the Department of Electrical Engineering, Nagaoka University of Technology, Niigata, Japan, as a research associate. From 2002 to 2003, he was a visiting scholar at the School of Mechanical Engineering, Purdue University, U.S.A. In 2004, he joined the Department of Electrical and Computer Engineering, Yokohama National University, Yokohama, Japan, as a lecturer and became an associate professor in 2005. Since 2010, he is an associate professor at the University of Tokyo. He received the Best Paper Award from the IEEE Transactions on Industrial Electronics in 2001 and 2013, Isao Takahashi Power Electronics Award in 2010, and Best Author Prize of SICE in 2010. His interests are in control engineering, motion control, nano-scale servo systems, electric vehicle control, and motor drive. Dr. Fujimoto is a member of IEEE, the Society of Instrument and Control Engineers, the Robotics Society of Japan, and the Society of Automotive Engineers of Japan.

Yoichi Hori (Fellow) received his B.S., M.S., and Ph.D. degrees in Electrical Engineering from the University of Tokyo, Tokyo, Japan, in 1978, 1980, and 1983, respectively. In 1983, he joined the Department of Electrical Engineering, the University of Tokyo, as a Research Associate. He later became an Assistant Professor, an Associate Professor, and, in 2000, a Professor at the same university. In 2002, he moved to the Institute of Industrial Science as a Professor in the Information and System Division, and in 2008, to the Department of Advanced Energy, Graduate School of Frontier Sciences, the University of Tokyo. From 1991–1992, he was a Visiting Researcher at the University of California at Berkeley. His research fields are control theory and its industrial applications to motion control, mechatronics, robotics, electric vehicles, etc. Prof. Hori is the winner of the Best Transactions Paper Award from the IEEE Transactions on Industrial Electronics in 1993, 2001, and 2013, of the 2000 Best Transactions Paper Award from the Institute of Electrical Engineers of Japan (IEEJ), and 2011 Achievement Award of IEE-Japan. He has been the Treasurer of the IEEE Japan Council and Tokyo Section since 2001. He is the past-President of the Industry Applications Society of the IEEJ, the President of Capacitors Forum, and the Chairman of Motor Technology Symposium of Japan Management Association (JMA), the Director on Technological Development of SAE-Japan (JSAE) and the Director of Japan Automobile Research Institute (JARI).

Yusuke Takeda (Non-member) received B.E. and M.E. degrees from the Department of Electrical and Electronic Engineering Systems, Utsunomiya University, Japan in 2008 and 2010, respectively. Since April 2010, he has been with ONO SOKKI CO., LTD. He works on the design of motion control of automotive-testing systems.

Koji Sato (Non-member) received B.E. and M.E. degrees from the Department of Mechanical and Control Engineering, the University of Electro-Communications, Japan in 1992 and 1994, respectively. Since April 1994, he has been with ONO SOKKI CO., LTD. He works on the design of motion control of automotive-testing systems.